

FIBRE-OPTIC COMMUNICATION

https://doi.org/10.1070/QEL16258

Nonlinear effects in optical signal transmission using a multimode fibre with weak coupling

O.S. Sidelnikov, A.A. Redyuk

Abstract. **We present the results of numerical simulation of nonlinear propagation of an optical signal in multimode gradient- and step-index fibres with weak coupling. It is found that when signals propagate in different modes, the system quality factor (*Q*-factor) for a gradient-index fibre increases with the number of the modes involved. The quality degradation of the transmitted data with increasing the number of the involved modes is demonstrated for the case when the signals in different modes travel at the same velocity. It is shown that the use of a step-index fibre may significantly deteriorate the signal quality due to the presence of a mode with a small dispersion parameter.**

Keywords: *multimode optical fibre, nonlinear effects, weak-coupling regime, numerical simulation.*

1. Introduction

To date, the use of fibre-optic communication lines is the most effective solution for transmitting large amounts of data over long distances. The exponentially growing demand for communication line capacity is the driving force for new research in the field of high-power optical data transmission systems. However, the transmission capacity of communication systems employing a conventional standard single-mode fibre (SSMF) is already approaching its limit due to the limited operating range of fibre amplifiers, high requirements to the signal-to-noise ratio, and restrictions imposed on the signal power launched into the fibre [1]. Currently, the annual traffic growth exceeds the growth in the net capacity of communication lines, and it is necessary to develop new technologies of data transmission to overcome this trend.

The development of communication systems based on multimode fibres (MMFs) is considered to be a promising way to solve this problem [2]. Multimode fibres can significantly increase the transmission capacity of optical networks owing to simultaneous signal transmission in different modes of a fibre. However, in the case of a simultaneous use of several modes, there arise new effects influencing the transmitted signals, such as linear mode coupling [3], differential group delay [4], and nonlinear intermode effects [5]. To successfully use multimode fibres as a medium allowing an increase in the data transfer rate, one should examine the impact of each of these effects.

To date, the results of laboratory experiments on the data transmission over six spatial modes for a 177-km MMF span are already presented [6]. The total line transmission capacity amounted to 24.6 Tbit s^{-1} at a spectral efficiency as large as 32 bit s^{-1} Hz^{-1}. In addition, a possibility of producing fibres capable of supporting 15 modes propagating simultaneously has been demonstrated [7]. Therefore, already at this stage of research, it is necessary to assess the impact of nonlinear intermode effects on the quality of transmitted signals as functions of the number of the modes used. In paper [8], the impact of nonlinear effects on signal propagation in multimode fibres in the regime of strong mode coupling is investigated. However, the model of strong coupling is not suitable for describing the nonlinear propagation in extended data transmission systems based on multimode fibres. In the present work, we consider the weak-coupling regime, which has been recently widely used in modelling multimode long-haul communication lines [9].

The paper presents the results of the research on the impact of nonlinear effects on the quality of transmitted signals with respect to the number of the modes involved. The cases of signal propagation in different modes with different and same velocities are analysed.

2. Mathematical model

The aim of this work is to establish the regularities and to assess the impact of nonlinear effects in multimode data transmission lines in the weak-coupling regime. To this end, a communication system shown schematically in Fig. 1 was used. Each transmitter generates 16-QAM signals with a symbol rate of R_s = 28.5 Gbaud, which, given the forward error correction FEC (14%), yields a bit rate of 100 Gbit s^{-1} in each mode. 16 quadrature amplitude modulation (16-QAM) is a type of signal amplitude modulation in which the carrier wave is divided into two identical-frequency carriers shifted relative to each other by 90°, with each of them being modulated by one of four discrete amplitude levels. Therefore, a single 16-QAM symbol transmits 4 bits of information. To form a pulse shape, a filter with a characteristic of 'raised cosine' type with a roll-off factor of 0.2 is used. The transmission line consists of 10 spans of multimode MMF fibre of 100 km each. At the end of each span, the signal attenuation is precisely compensated for by means of EDFA erbium optical amplifiers with an amplifier noise factor NF = 4.5. The noise corresponding to the amplified spontaneous emission of the amplifiers is added to the optical signal after each span.

O.S. Sidelnikov, A.A. Redyuk Novosibirsk State University, ul. Pirogova 2, 630090 Novosibirsk, Russia; Institute of Computational Technologies, Siberian Branch, Russian Academy of Sciences, prosp. Akad. Lavrent'eva 6, 630090 Novosibirsk, Russia; e-mail: alexey.redyuk@gmail.com, o.s.sidelnikov@gmail.com

Received 23 November 2016; revision received 6 February 2017
Kvantovaya Elektronika **47** (4) 330–334 (2017)
Translated by M.A. Monastyrskiy

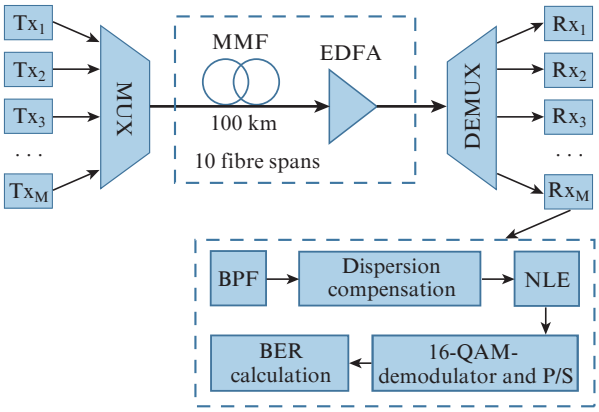

Figure 1. Scheme of the line in question:
(Tx) signal transmitter for a single mode; (MUX) mode multiplexer; (EDFA) erbium-doped fibre amplifier; (DEMUX) mode demultiplexer; (Rx) signal receiver for a single mode; (BPF) bandpass filter; (NLE) nonlinear effect compensation.

Chromatic dispersion and differential group delays are precisely compensated for in digital form during the optical signal passage through the Rx receiver. To compensate for the nonlinear effects for each received mode, a procedure based on the support vector machine (SVM) is employed [10]. To evaluate the system performance, the Q-factor averaged over all the modes is calculated, which is related to the bit error rate (BER) as follows:

$$\mathrm{BER} = \frac{1}{2}\,\mathrm{erfc}\left(\frac{Q}{\sqrt{2}}\right),$$

where BER is the ratio of the number of erroneously received bits to the total number of transmitted bits. Thus, the Q-factor is an indicator of the transmitted signal quality in each mode; in this case, the higher the Q-factor, the less problems occur in data transmission.

The impact of nonlinear effects on the propagation of optical signals in multimode fibres is investigated as a function of the number of modes that are used in the weak-coupling regime. This regime is characterised by the fact that the linear coupling between various spatial modes is small compared to that between two polarisation components of a single spatial mode (in the case of a strong coupling mode both quantities are of the same order). Thus, nonlinear signal propagation over a single mode of a multimode fibre is described by the Manakov equation [11]:

$$\frac{\partial \bar{A}_p}{\partial z} + \langle \delta\beta_{0p}\rangle \bar{A}_p + \langle \delta\beta_{1p}\rangle \frac{\partial \bar{A}_p}{\partial t} + \mathrm{i}\frac{\beta_{2p}}{2}\frac{\partial^2 \bar{A}_p}{\partial t^2}$$
$$= \mathrm{i}\gamma\left(f_{pppp}\frac{8}{9}|\bar{A}_p|^2 + \sum_{m\neq p} f_{mmpp}\frac{4}{3}|\bar{A}_m|^2\right)\bar{A}_p, \qquad (1)$$

where

$$\langle \delta\beta_{0p}\rangle = \frac{1}{2}(\beta_{px} + \beta_{py}) - \beta_{\mathrm{g}},$$

$$\langle \delta\beta_{1p}\rangle = \frac{1}{2}\left(\frac{\partial\beta_{px}}{\partial\omega}\Big|_{\omega_0} + \frac{\partial\beta_{py}}{\partial\omega}\Big|_{\omega_0}\right) - \frac{1}{v_g}.$$

Here β_{0p}, β_{1p} and β_{2p} are the propagation constant, inverse group velocity, and group velocity dispersion of the spatial pth mode, respectively; β_{g} and v_{g} are the propagation constant and group velocity of the fundamental mode; $\gamma = \omega_0 n_2/(cA_{\mathrm{eff}})$ is a nonlinear parameter, where n_2 is the nonlinear index of glass refraction, and A_{eff} is the fundamental mode effective area at the centre frequency ω_0; and f_{lmnp} is the nonlinear coupling coefficient for spatial modes, which has the form:

$$f_{lmnp} = \frac{A_{\mathrm{eff}}}{\sqrt{I_l I_m I_n I_p}}\iint F_l F_m F_n F_p \,\mathrm{d}x\,\mathrm{d}y, \qquad (2)$$

where F_p is the spatial distribution of the mode p; $I_p = (\bar{n}_p/\bar{n}_{\mathrm{eff}})\iint |F_p|^2(x,y)\,\mathrm{d}x\,\mathrm{d}y$; and n_{eff} and n_{p} are the effective refractive indices of the fundamental mode and mode p, respectively.

The SVM method used in our work is similar to the approach presented in [10], where a multi-class classification model is used, capable of recognising different 16-QAM symbols. To construct nonlinear class separators, a radial basis function with a parameter $\gamma_{\mathrm{SVM}} > 0$ is used as a core. Cross-validation is also used in the frame of the SVM method to find the best γ_{SVM} and the regularisation parameter C. Then, using these parameters, the SVM detector is trained using the received 2^{12} 16-QAM symbols. After training, this SVM detector is used in the numerical experiments for the recognition of the received signal.

3. Results of numerical simulation

To numerically solve the Manakov equation (1), a symmetric variant of the split-step Fourier method was used, which has the second-order accuracy with respect to the step h of the evolutionary variable z. The propagation equations for each of the modes were solved numerically with a step of 100 m. In the calculations, we checked that a further decrease in the numerical step did not change the results.

As a channel for signal transmission, we used a multimode fibre having a graded-core (the gradient index, $a_{\mathrm{gr}} = 2$) with a cladding trench (GCCT) profile. This fibre is currently used to lower down the differential mode delay in the propagation of multiple modes, which is necessary to reduce the complexity of MIMO receivers [12]. The GCCT profile of the fibre is shown in Fig. 2 and is described analytically as

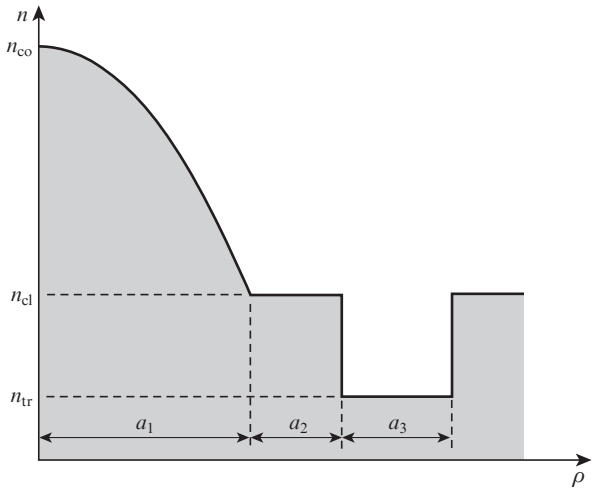

Figure 2. Refractive index profile of the GCCT fibre.

$$n(\rho) = \begin{cases} n(0)[1 - \Delta n_{co}(\rho/a_1)^{\alpha_{gr}}], & |\rho| < a_1, \\ n_{cl}, & a_1 < |\rho| < a_1 + a_2, \\ n_{tr}, & a_1 + a_2 < |\rho| < a_1 + a_2 + a_3, \\ n_{cl}, & |\rho| > a_1 + a_2 + a_3. \end{cases}$$

In our numerical experiments, the following fibre profile parameters were used: core/cladding refractive indices n_{co} = 1.4559 and n_{cl} = 1.444, respectively; a_1 = 15 μm; a_2 = 1 μm; refractive index of the trench n_{tr} = 1.44; and a_3 = 4 μm [13]. Such a fibre allows the propagation of nine spatial modes except for those degenerated (LP_{01}, LP_{11}, LP_{02}, LP_{21}, LP_{12}, LP_{31}, LP_{22}, LP_{41}, and LP_{03}).

In modelling the signal propagation we have taken into account that the fibre losses are equal to α = 0.2 dB km^{-1}, the fibre nonlinearity is γ = 1.4 W^{-1} km^{-1}, the carrier wavelength of a single-channel signal is λ = 1550 nm, the number of samples per each symbol is q = 16, and the total number of symbols is $N_s = 2^{18}$. The values of differential mode delay (DMD), dispersion (D), and effective mode area for each mode are given in Table 1. The coefficients of the nonlinear coupling between all spatial the modes are given in Table 2, the lower part of which is not filled because $f_{mmpp} = f_{ppmm}$.

Table 1. Differential mode delay, dispersion, and effective mode area for the GCCT fibre.

Mode	DMD/ps km^{-1}	D/ps (km nm)$^{-1}$	A_{eff}/μm^2
LP_{01}	0	20.2	129.9
LP_{11}	19.6	20.4	168.7
LP_{02}	35.4	20.5	250.4
LP_{21}	42.6	20.6	224.5
LP_{12}	26.5	20.5	270.7
LP_{31}	59.4	20.6	269.2
LP_{22}	–111.3	19.2	341.9
LP_{41}	38.7	20.5	308.6
LP_{03}	–187.7	18.4	364

Table 2. Coefficients of nonlinear coupling between the spatial modes for the GCCT fibre.

Mode	LP_{01}	LP_{11}	LP_{02}	LP_{21}	LP_{12}	LP_{31}	LP_{22}	LP_{41}	LP_{03}
LP_{01}	1	0.4976	0.5094	0.2483	0.3736	0.1238	0.2462	0.0616	0.3847
LP_{11}		0.7547	0.2508	0.3780	0.3770	0.2519	0.2492	0.1569	0.1862
LP_{02}			0.5110	0.2511	0.2520	0.2513	0.1250	0.2194	0.3240
LP_{21}				0.5692	0.1897	0.3166	0.2817	0.2369	0.1551
LP_{12}					0.4734	0.1908	0.2201	0.1988	0.1729
LP_{31}						0.4759	0.1578	0.2774	0.1404
LP_{22}							0.3757	0.1589	0.1865
LP_{41}								0.4164	0.1411
LP_{03}									0.3542

Figure 3a shows the Q-factor at the receiver, averaged over all the modes involved, as a function of the initial signal power in a single mode when signals propagate over one, two, three, six, or nine modes of the GCCT fibre. One can see that the transmitted signal quality increases with increasing number of modes, reaching a difference of 1 dB for the cases with one and nine modes.

To explain this effect, consider Fig. 3b, which shows the Q-factor only for the LP_{01} mode as a function of the initial signal power when transmitting data using one, two, three, and nine modes. In this case, in all calculations we evaluated not the Q-factor averaged over all the modes, but its value for

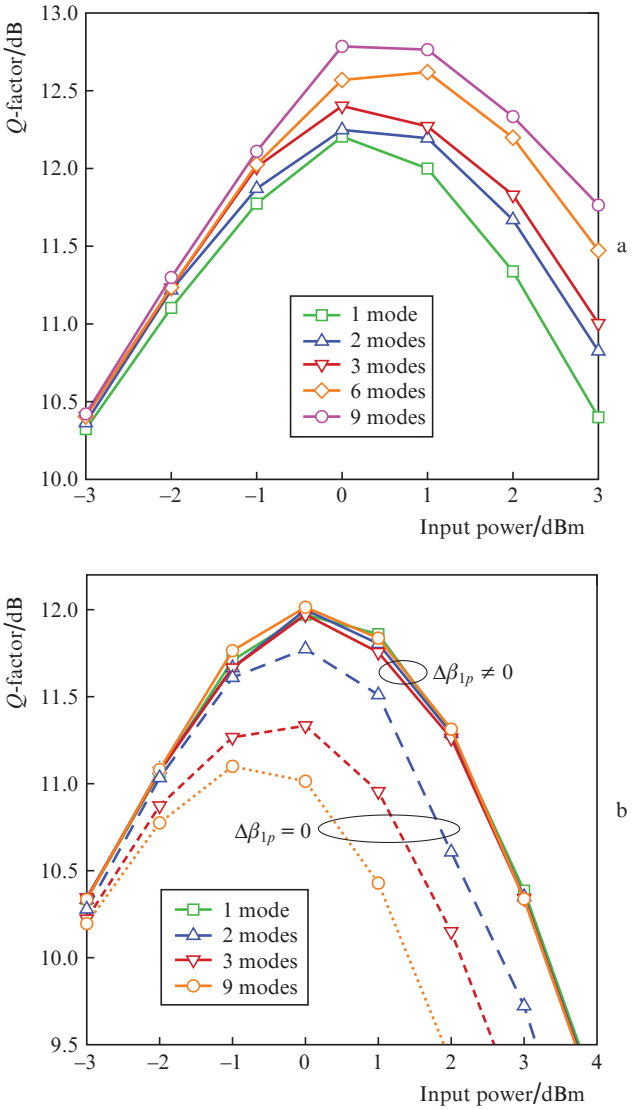

Figure 3. Q-factor averaged over all the modes (a) and calculated only for the LP_{01} mode (b) as a function of the initial signal power for the GCCT fibre.

the LP_{01} mode. As can be seen from the figure, if the group velocities of all the modes are different (solid line, $\Delta\beta_{1p} \neq 0$), the Q-factor for the LP_{01} mode is virtually unchanged when adding new modes. This is due to the fact that for the fibres used, the signals in the modes propagate with slightly different velocities; therefore, the pulses in different modes move relative to each other, and the nonlinear intermode interaction between them virtually does not affect the transmitted signal quality in the LP_{01} mode even with increasing number of the modes involved. An illustration of this effect is shown in Fig. 4a. If all the modes move at the same velocity (dotted lines, $\Delta\beta_{1p} = 0$), the signal for the mode LP_{01} turns out significantly degraded when adding the new modes, which is caused by an additional nonlinear intermode interaction (Fig. 4b).

In our study we have found that this observation is fulfilled for each of the propagating modes. Thus, the nonlinear signal distortions in each mode are only due to the first term in the right-hand side of Eqn (1), with a coefficient f_{pppp} in front of it. However, as can be seen from Table 2, these coefficients decrease with increasing mode order. Therefore, each time when a new mode of higher order is added, it suf-

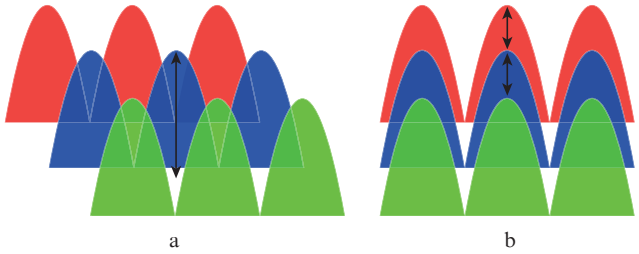

Figure 4. Distribution of various modes in a multimode fibre with (a) different and (b) same velocities.

fers a lesser nonlinear distortion, and the Q-factor of that mode will be higher compared to the previous modes. Therefore, the Q-factor averaged over all the modes increases with increasing number of the modes involved, which can be seen from Fig. 3a.

Figure 5 shows the dependence of the Q-factor averaged over all the modes involved on the initial signal power during its propagation over one, two, three, six, or nine modes of a multimode GCCT fibre in the case when the signals in different modes travel with the same velocity ($\Delta\beta_{1p} = 0$). It is seen that, with increasing number of modes up to three, the Q-factor decreases as expected (see Fig. 3b), because all the modes are subjected to a stronger impact of the intermode nonlinearity. However, with a further increase in the number of modes, the Q-factor increases slightly because, for the higher-order modes, the nonlinear coefficients f_{mmpp} (responsible for the intermode interaction) and the coefficients f_{pppp} are small, so that the modes in lesser degree are susceptible to nonlinear effects. It should be noted that even when only five modes are involved, addition of each succeeding mode has virtually no effect on the result.

This paper also investigates a step-index fibre with the parameters $n_{co} = 1.454$, $n_{cl} = 1.444$, $a_1 = 7$ μm. Such fibres allows the propagation of four modes (LP_{01}, LP_{11}, LP_{02}, and LP_{21}). The differential mode delay, dispersion, and effective mode area for each mode of such a fibre are presented in Table 3. The coefficients of the nonlinear coupling between all the spatial modes of a step-index fibre are given in Table 4.

Table 3. Differential mode delay, dispersion, and effective mode area for a step-index fibre.

Mode	DMD/ps km^{-1}	D/ps (km nm)$^{-1}$	A_{eff}/μm^2
LP_{01}	0	22.5	102
LP_{11}	4.2	23.2	103
LP_{02}	6.1	3.3	121.4
LP_{21}	7.9	17.2	122

Table 4. Coefficients of nonlinear coupling between spatial modes for a step-index fibre.

Mode	LP_{01}	LP_{11}	LP_{02}	LP_{21}
LP_{01}	1	0.6294	0.6871	0.4068
LP_{11}		0.9932	0.3283	0.5585
LP_{02}			0.8474	0.2934
LP_{21}				0.8425

Figure 6 shows the Q-factor averaged over all the modes involved as a function of the initial signal power in the propagation of optical signals over one, two, three, or four modes of the step-index fibre. As can be seen from the figure, the Q-factor is nearly the same for the cases of one or two modes, but adding a signal propagating over the third mode (LP_{02}) degrades significantly the system performance. This is explained by the fact that the dispersion parameter is small for the LP_{02} mode [3.34 ps (km nm)$^{-1}$], so that the signal propagating in this mode suffers lesser dispersion broadening and, consequently, is more susceptible to nonlinear distortions. Thus, the contribution of the LP_{02} mode to the Q-factor averaged over all the modes involved degrades the signal quality. The situation can be slightly improved by adding the fourth mode (LP_{21}) with a sufficiently large dispersion parameter. In this case, the Q-factor exceeds the relevant value reached in the case of the three modes.

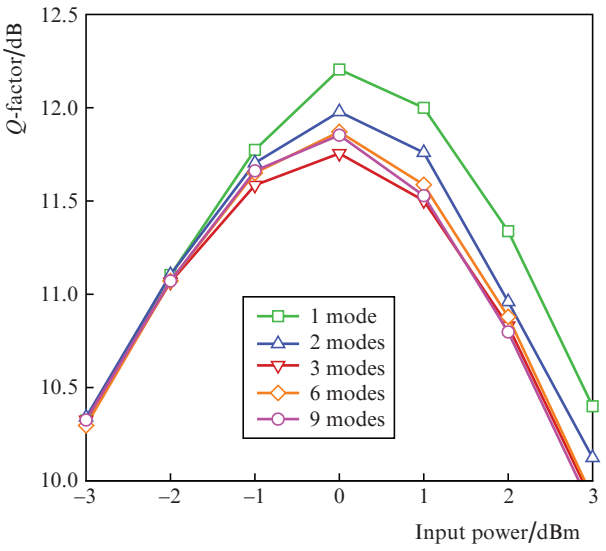

Figure 5. Q-factor as a function of the initial signal power for the GCCT fibre at $\Delta\beta_{1p} = 0$.

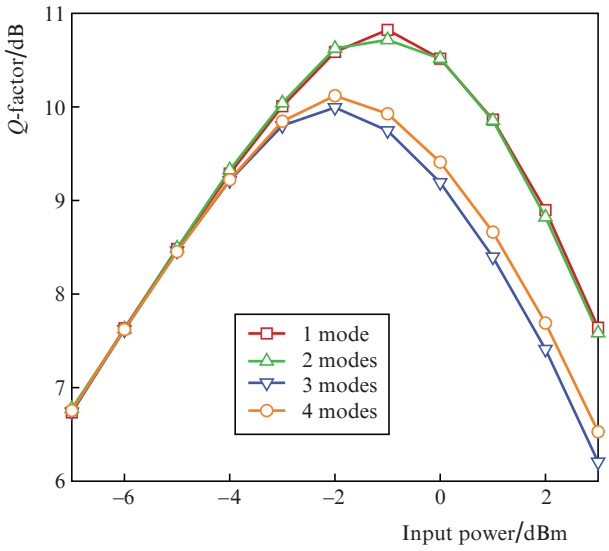

Figure 6. Q-factor as a function of the initial signal power for a step-index fibre.

4. Conclusions

Thus, we have performed a mathematical modelling of the evolution of optical signals in multimode fibres in the framework of a model based on the Manakov equations in the weak-coupling regime. For this purpose, a numerical algorithm based on the split-step Fourier method has been implemented.

We have studied the impact of nonlinear effects on the system performance in an optical communication system based on the use of multimode fibres having a graded-core with a cladding trench profile. For this fibre, an increase in the Q-factor with increasing number of the modes involved is demonstrated and justified. We also have considered the case when all the modes travel at the same velocity, and have shown the degradation of the transmitted signal quality with increasing number of the modes, which is caused by the intermode nonlinearity.

A step-index fibre which allows the propagation of a mode with a small dispersion parameter has been investigated. It is shown that a signal propagating in this mode is in greater degree susceptible to nonlinear distortions, and the presence of this mode may significantly deteriorate the average value of the Q-factor.

Acknowledgements. The work of A.A.R. was supported by the Russian Science Foundation (Project No. 14-21-00110), the work of O.S.S. was supported by the RF President's Grants Council (State Support of Young Russian Scientists Programme, Grant No. MK-9240.2016.9).

References

1. Tkach R. *Bell Labs Tech. J.*, **14**, 4 (2010).
2. Ryf R. et al. *Proc. OFC/NFOEC* (Los Angeles, CA, USA, 2011) paper PDPB10.
3. Marcuse D. *Theory of Dielectric Optical Waveguides* (New York: Acad., 1991).
4. Ho K. et al. *J. Lightwave Technol.*, **29**, 21 (2011).
5. Rademacher G. et al. *Photon. Technol. Lett.*, **24**, 21 (2012).
6. Ryf R. et al. *Proc. OFC/NFOEC* (Anaheim, CA, USA, 2013) paper PDP5A.1.
7. Sillard P. et al. *Proc. OFC/NFOEC* (Los Angeles, CA, USA, 2015) paper M2C.2.
8. Brehler M. et al. *Proc. OFC/NFOEC* (Anaheim, CA, USA, 2016) paper W4I.3.
9. Rademacher G. et al. *Opt. Express*, **23**, 1 (2015).
10. Nguyen T. et al. *IEEE Photon. J.*, **8**, 2 (2016).
11. Mumtaz S. et al. *J. Lightwave Technol.*, **31**, 3 (2013).
12. Inan B. et al. *Proc. OFC/NFOEC* (Los Angeles, CA, USA, 2012) paper OW3D.4.
13. Ferreira F.M. et al. *J. Lightwave Technol.*, **32**, 3 (2014).